Title
Monovalent permeability, rectification, and ionic block of store-operated calcium channels in Jurkat T lymphocytes.

Journal
The Journal of general physiology, 111(4)

ISSN
0022-1295

Authors
Kerschbaum, HH
Cahalan, MD

Publication Date
1998-04-01

DOI
10.1085/jgp.111.4.521

Peer reviewed

Monovalent Permeability, Rectification, and Ionic Block of Store-operated Calcium Channels in Jurkat T Lymphocytes

HUBERT H. KERSCHBAUM*‡ and MICHAEL D. CAHALAN*

From the *Department of Physiology and Biophysics, University of California, Irvine, California 92697; and ‡Department of Animal Physiology, University of Salzburg, Institute for Zoology, A-5020 Salzburg, Austria

ABSTRACT We used whole-cell recording to characterize ion permeation, rectification, and block of monovalent current through calcium release-activated calcium (CRAC) channels in Jurkat T lymphocytes. Under physiological conditions, CRAC channels exhibit a high degree of selectivity for Ca^{2+}, but can be induced to carry a slowly declining Na^+ current when external divalent ions are reduced to micromolar levels. Using a series of organic cations as probes of varying size, we measured reversal potentials and calculated permeability ratios relative to Na^+, P_X/P_{Na}, in order to estimate the diameter of the conducting pore. Ammonium (NH_4^+) exhibited the highest relative permeability ($P_{NH4}/P_{Na} = 1.37$). The largest permeant ion, tetramethylammonium with a diameter of 0.55 nm, had P_{TMA}/P_{Na} of 0.09. *N*-methyl-D-glucamine ($0.50 \times 0.64 \times 1.20$ nm) was not measurably permeant. In addition to carrying monovalent current, NH_4^+ reduced the slow decline of monovalent current ("inactivation") upon lowering $[Ca^{2+}]_o$. This kinetic effect of extracellular NH_4^+ can be accounted for by an increase in intracellular pH (pH_i), since raising intracellular pH above 8 reduced the extent of inactivation. In addition, decreasing pH_i reduced monovalent and divalent current amplitudes through CRAC channels with a pK_a of 6.8. In several channel types, Mg^{2+} has been shown to produce rectification by a voltage-dependent block mechanism. Mg^{2+} removal from the pipette solution permitted large outward monovalent currents to flow through CRAC channels while also increasing the channel's relative Cs^+ conductance and eliminating the inactivation of monovalent current. Boltzmann fits indicate that intracellular Mg^{2+} contributes to inward rectification by blocking in a voltage-dependent manner, with a $z\delta$ product of 1.88. Ca^{2+} block from the outside was also found to be voltage dependent with $z\delta$ of 1.62. These experiments indicate that the CRAC channel, like voltage-gated Ca^{2+} channels, achieves selectivity for Ca^{2+} by selective binding in a large pore with current–voltage characteristics shaped by internal Mg^{2+}.

KEY WORDS: calcium channel • CRAC channel • I_{CRAC} • ion selectivity • inward rectification

INTRODUCTION

Stimulation of T lymphocytes by antigen-presenting cells initiates a cascade of events, including tyrosine phosphorylation and activation of phospholipase C, resulting in the release of Ca^{2+} from intracellular IP_3-sensitive stores and an increase of cytoplasmic Ca^{2+} concentration $[Ca^{2+}]_i$ (Crabtree and Clipstone, 1994). The increase in $[Ca^{2+}]_i$ is sustained by influx of Ca^{2+} through Ca^{2+} channels located in the plasma membrane. Sustained elevations or long-lasting oscillatory changes in $[Ca^{2+}]$ are essential for proliferation and gene expression in T cells (Negulescu et al., 1994; Fanger et al., 1995; reviewed by Lewis and Cahalan, 1995). The most extensively investigated mechanism for Ca^{2+} influx in T cells is a stores-operated Ca^{2+} channel, known as the Ca^{2+} release-activated Ca^{2+} (CRAC)[1] channel. CRAC channels with a high degree of selectivity for Ca^{2+} are observed in lymphocytes and mast cells (Lewis and Cahalan, 1989; Hoth and Penner, 1992; Zweifach and Lewis, 1993), while numerous other cell types possess similar Ca^{2+}-permeable channels activated by Ca^{2+} store depletion. Regardless of the initiating stimulus (surface receptor engagement, passive dialysis of the cytoplasm with Ca^{2+} buffer, direct addition of IP_3 to empty IP_3-sensitive stores, addition of the Ca^{2+} ionophore ionomycin, or inhibition of the Ca^{2+}-ATPase uptake pump with thapsigargin), depletion of Ca^{2+} from intracellular stores activates CRAC channels through an unknown mechanism (Lewis and Cahalan, 1989; Hoth and Penner, 1992; Zweifach and Lewis, 1993; Premack et al., 1994; Zhang and McCloskey, 1995). The resulting Ca^{2+} current (I_{CRAC}) is not voltage dependent in its gating, but exhibits inward rectification and a very positive reversal potential. The primary mechanism of activation after depletion of intracellular Ca^{2+} stores is not well defined, but channel gating is known to be regulated by $[Ca^{2+}]_i$, and by kinases and nucleotides (reviewed in Parekh and Penner, 1996; Lewis et al., 1996). The focus of this paper is ion permeation through CRAC channels.

Address correspondence to Michael D. Cahalan, Department of Physiology and Biophysics, University of California, Irvine, CA 92697-4560. Fax: 714-824-3143; E-mail: mcahalan@uci.edu

[1]*Abbreviations used in this paper:* CRAC, calcium release-activated calcium; I-V, current–voltage; $NMDG^+$, *N*-methyl-D-glucamine; TMA^+, tetramethylammonium.

Under physiological conditions, CRAC channels are highly selective for Ca^{2+}, enabling a very small current (~1 pA/pF at −80 mV in Jurkat T cells) to support the $[Ca^{2+}]_i$ signal (Lewis and Cahalan, 1989; Hoth and Penner, 1992; Zweifach and Lewis, 1993; Hoth, 1995). Reducing external divalents to the micromolar range reveals a much larger monovalent current through CRAC channels, carried by Na^+ in low divalent Ringer or by other alkali cations in test solutions (Hoth and Penner, 1993; Premack et al., 1994; Lepple-Wienhues and Cahalan, 1996). In the absence of external Mg^{2+}, the Na^+ current through CRAC channels immediately after lowering $[Ca^{2+}]_o$ peaks at a value ~5–10-fold larger than the preceding Ca^{2+}-selective current, and then declines by an unknown mechanism. Although differing fundamentally in gating (store depletion vs. depolarization to open the channel), CRAC channels and voltage-gated Ca^{2+} channels exhibit a similar loss of selectivity upon lowering $[Ca^{2+}]_o$, and in both channel types selection against monovalents can be ascribed to the binding of Ca^{2+} ions with micromolar affinity to sites within the channel conduction pathway (Hess and Tsien, 1984; Almers and McCleskey, 1984; Lepple-Wienhues and Cahalan, 1996). Based on analysis of conductance fluctuations, CRAC channels have an extremely small unitary conductance of 24 fS in high $[Ca^{2+}]_o$ (Zweifach and Lewis, 1993), but the conductance of CRAC channels carrying Na^+ is ~100 times larger, compatible with a channel mechanism of ion permeation (Lepple-Wienhues and Cahalan, 1996). Under similar ionic conditions, the single-channel conductance of L-type voltage-gated Ca^{2+} channels is ~300× larger than that of CRAC channels (Zweifach and Lewis, 1993; Hess et al., 1986).

Although CRAC channels and voltage-gated Ca^{2+} channels differ in their gating behavior and unitary conductance, they share a high degree of divalent selectivity and exhibit similar affinities for Ca^{2+}. This could indicate that both channels share similar structural features necessary for Ca^{2+} selectivity. Recently, the *Drosophila trp* (transient receptor potential) gene and its mammalian homologs have been proposed to mediate stores-dependent Ca^{2+} entry, although *trp* genes expressed in cell lines exhibit different selectivity properties, including rather low selectivity for Ca^{2+} over monovalent ions compared with the CRAC channel with normal levels of extracellular Ca^{2+} (Vaca et al., 1994; Zhu et al., 1996; Zitt et al., 1996; reviewed by Clapham, 1996). One motivation for further characterizing the selectivity properties of the CRAC channel is to facilitate identification of the gene encoding this physiologically important channel by comparison with the selectivity properties of expressed candidate genes.

This paper addresses properties of CRAC channels that are related to ion selectivity, rectification, and block: the physical size of the pore, its conduction properties as a function of intracellular pH, the Mg^{2+} dependence of inward rectification, and the Ca^{2+} dependence of current. In addition, we show that the decline of monovalent current through CRAC channels can be prevented by reducing the concentration of cytoplasmic protons or Mg^{2+} ions. We conclude that the CRAC channel is a large pore that achieves selectivity for Ca^{2+} by selective binding of external Ca^{2+}, with current–voltage (I-V) rectification influenced by internal Mg^{2+}.

METHODS

Cell Culture

The human T cell line, Jurkat E6-1 was cultured in RPMI 1640 with 10% fetal calf serum, 1 mM glutamine, and 25 mM HEPES in a 5% CO_2 incubator at 37°C.

Whole-Cell Recordings

Patch clamp experiments were performed at room temperature in the standard whole-cell recording configuration (Hamill et al., 1981). Pipettes were pulled from soft glass capillaries (Accu-fill 90 Micropets; Becton Dickinson and Co., Parsippany, NJ), coated with Sylgard (Dow Corning Corp., Midland, MI), and fire polished to a resistance of 2–5 MΩ when filled with internal solutions. Membrane currents were recorded using an EPC-9 patch-clamp amplifier (HEKA, Lambrecht, Germany). Data were sampled at a rate of 5–10 kHz and digitally filtered at 0.7 kHz for analysis and display. Fast and slow capacitative transients were canceled by the compensation circuitry of the EPC-9. The membrane capacitance of cells selected for recording was 6.3 ± 1.8 (n = 300). Command potentials were corrected for liquid junction potentials. The series resistance (4–10 MΩ) was not compensated. The membrane potential was clamped at 0 mV, and 200-ms voltage ramps from −120 to +50 mV were delivered every second. Leak currents before activation of CRAC channels were averaged and subtracted from subsequent current records. With Cl^- replacement, input resistances determined before store depletion were >10 GΩ. I_{CRAC} was induced by passive Ca^{2+} store depletion using 12 mM BAPTA. External solutions were changed by puffer pipettes as described (Lepple-Wienhues and Cahalan, 1996).

Solutions

Methanesulfonate was the main anion in the external solution, to reduce the permeability through Cl^- channels (Lewis et al., 1993). For measurement of relative permeabilities, Na^+ in the bathing solution was replaced by alkylated ammonium derivatives (see below). EGTA and HEDTA saturated with Ca^{2+} were prepared using a pH–metric method (Neher, 1988). The low $[Ca^{2+}]_o$ external solution had the following composition (mM): 150 X^+, 150 methane sulfonate, 2 mM EGTA, where X^+ is Na^+, K^+, Li^+, Cs^+, NH_4^+, methylammonium, dimethylammonium, trimethylammonium, tetramethylammonium (TMA^+), ethylammonium, isopropylammonium, hydrazine, or *N*-methyl-D-glucamine ($NMDG^+$). External solutions containing various $[Ca^{2+}]_o$ were buffered with 2 mM HEDTA (1 μM, 10 μM free Ca^{2+}) or with 2 mM EGTA (1 μM, 0.1 μM free Ca^{2+}). Nominally divalent-free solution contained 150 mM Na^+ methane sulfonic acid. All solutions contained 10 mM HEPES. The osmolarity was adjusted to

300 mosmol with glucose, and the pH was titrated to pH 7.2. NH_4^+, methylamine, dimethylamine, trimethylamine, and TMA^+ were purchased from Aldrich Chemical Co. (Milwaukee, WI); ethylamine, isopropylamine, hydrazine, and methane sulfonic were purchased from Sigma Chemical Co. (St. Louis, MO).

The pipette solution usually contained (mM): 128 Cs aspartate, 10 Cs-HEPES, 12 BAPTA, 0.9 $CaCl_2$, 3.16 $MgCl_2$, pH 7.2. In some pipette solutions, Cs^+ ions were substituted by Na^+ or $NMDG^+$. Solutions titrated to 6.2 and 6.8 sometimes contained 10 mM Tris instead of HEPES. In Mg^{2+}- free solutions, $MgCl_2$ was omitted from the internal solution.

RESULTS

CRAC Channels are Permeable to Monovalent Cations when External Ca^{2+} Is Lowered

In physiological solutions with external Ca^{2+} concentration ($[Ca^{2+}]_o$) in the millimolar range, CRAC channels are highly selective for Ca^{2+} over monovalent cations. However, previous studies have shown that when external divalents are reduced to the micromolar range, Na^+ ions carry a large, transient inward current through CRAC channels (Hoth and Penner, 1993; Lepple-Wienhues and Cahalan, 1996). In the present study, we activated CRAC channels by dialyzing the cell with BAPTA-buffered low $[Ca^{2+}]_i$ solutions ($[Ca^{2+}]_{free}$ = 5 nM) to deplete intracellular Ca^{2+} stores passively. Currents were recorded during 200-ms voltage ramps from −120 to +50 mV delivered every second. In the presence of high $[Ca^{2+}]_o$, a small inwardly rectifying Ca^{2+} current (I_{CRAC}) was induced during dialysis (Fig. 1, *A–C*). In the absence of external Mg^{2+} and immediately upon reducing $[Ca^{2+}]_o$ to 1 μM, a large inwardly rectifying Na^+ current developed, and then slowly declined over tens of seconds (Fig. 1 *D*). This current was carried by Na^+ since it vanished when $NMDG^+$ was substituted for Na^+ in the bath. Similar large monovalent currents were observed in cells dialyzed with Cs^+, Na^+, or $NMDG^+$ (Fig. 1, *A–C*), but only if CRAC channels were already activated by Ca^{2+} store depletion during dialysis. The parallel development of monovalent and Ca^{2+} current during the initial phase of CRAC channel activation provides evidence that the monovalent current is carried through CRAC channels, rather than through a nonspecific "leak" (Lepple-Wienhues and Cahalan, 1996). With $NMDG^+$ as the main internal cation, the current density measured at −80 mV was 0.8 ± 0.2 pA/pF (n = 4) when the channel

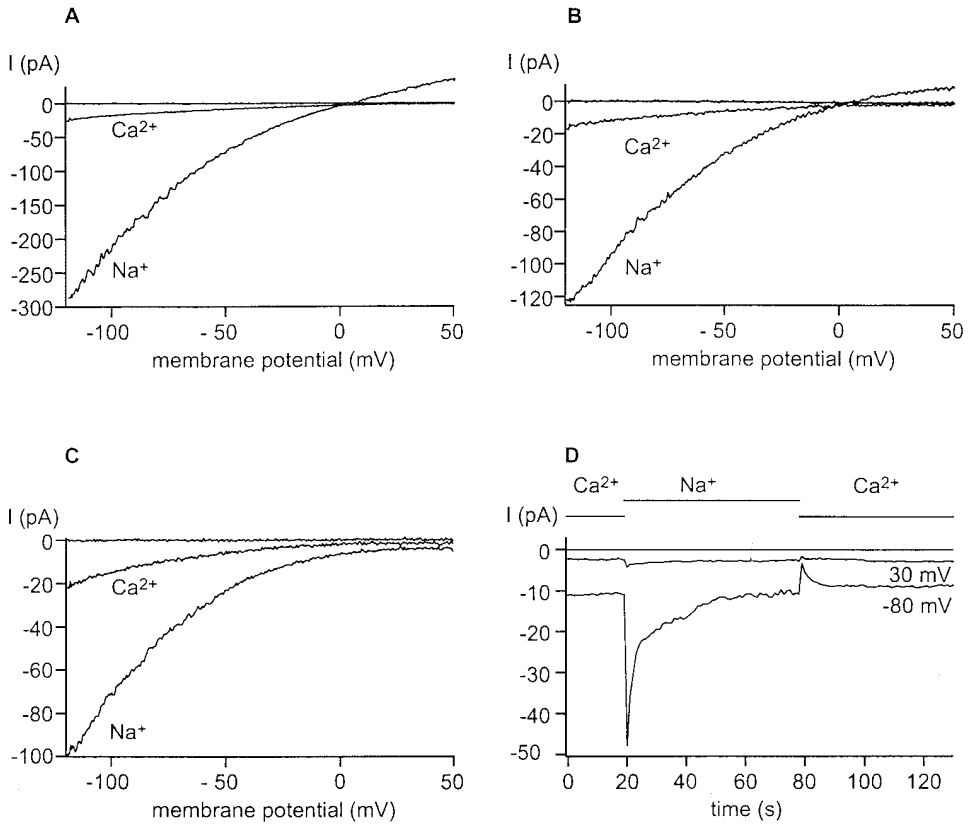

FIGURE 1. Divalent and monovalent current through CRAC channels. CRAC channels were activated during dialysis with Na^+ (*A*), Cs^+ (*B*), or $NMDG^+$ (*C*) aspartate pipette solutions. The superfusion solution was changed from 20 mM to 1 μM Ca^{2+} to induce monovalent current through CRAC channels. Currents were recorded during 200-ms voltage ramps from −120 to +50 mV delivered every second, using a holding potential of 0 mV. Sweeps depicted in *A–C* represent a current trace with 20 mM Ca^{2+} before CRAC channels activate, and following activation of CRAC channels using Ca^{2+} or Na^+ as the current carrier. Ca^{2+} and Na^+ currents through CRAC channels rectify inwardly. Small outward currents carried by Na^+ (*A*) or Cs^+ (*B*) can also be observed at positive voltages when $[Ca^{2+}]_o$ is lowered. $NMDG^+$ does not carry detectable outward currents (*C*). (*D*) Amplitude of the divalent and monovalent current through CRAC channels at −80 and +30 mV plotted against time using $NMDG^+$ as internal cation. The bar indicates the main current carrier; note that the Na^+ current declines after peaking when $[Ca^{2+}]_o$ is reduced to 1 μM.

carried Ca^{2+} in 20 mM Ca^{2+}, and the peak Na current upon lowering Ca^{2+} to 1 μM was 3.7 ± 0.7 pA/pF (n = 4). The ratio of monovalent to divalent current indicates that the CRAC channel can conduct monovalent ions much more readily than Ca^{2+} ions. Later in this paper, we show that the measured monovalent to divalent current ratio is even higher if the decline of monovalent current upon $[Ca^{2+}]_o$ removal is prevented.

Although varying the internal or external monovalent ionic species did not affect the development of the monovalent current, reversal potentials and current magnitudes through CRAC channels depended upon the current-carrying species. At positive potentials, a small outward current was observed in low $[Ca^{2+}]_o$ using Cs^+- or Na^+-containing internal solutions (Fig. 1, *A* and *B*). This outward current was carried by Cs^+ or Na^+ through CRAC channels, since it activated with the same time course as the inward current, was blocked by La^{3+}, and was not present in experiments using $NMDG^+$ in the internal solution (Fig. 1 *C*). Upon lowering $[Ca^{2+}]_o$, inward current magnitudes varied substantially depending upon the external species of monovalent cation. For example, Na^+ carried a much larger inward current through CRAC channels than Cs^+ did; the ratio of Na^+ to Cs^+ inward currents was 26 ± 3 (SD; n = 5), even though the measured reversal potentials were similar and outward Na^+ and Cs^+ currents were of comparable magnitude. $NMDG^+$ inward current could not be detected.

These results verify and extend a previous report (Lepple-Wienhues and Cahalan, 1996) that, under conditions of low $[Ca^{2+}]_o$, CRAC channels become permeable to monovalent cations, a property shared with volt-

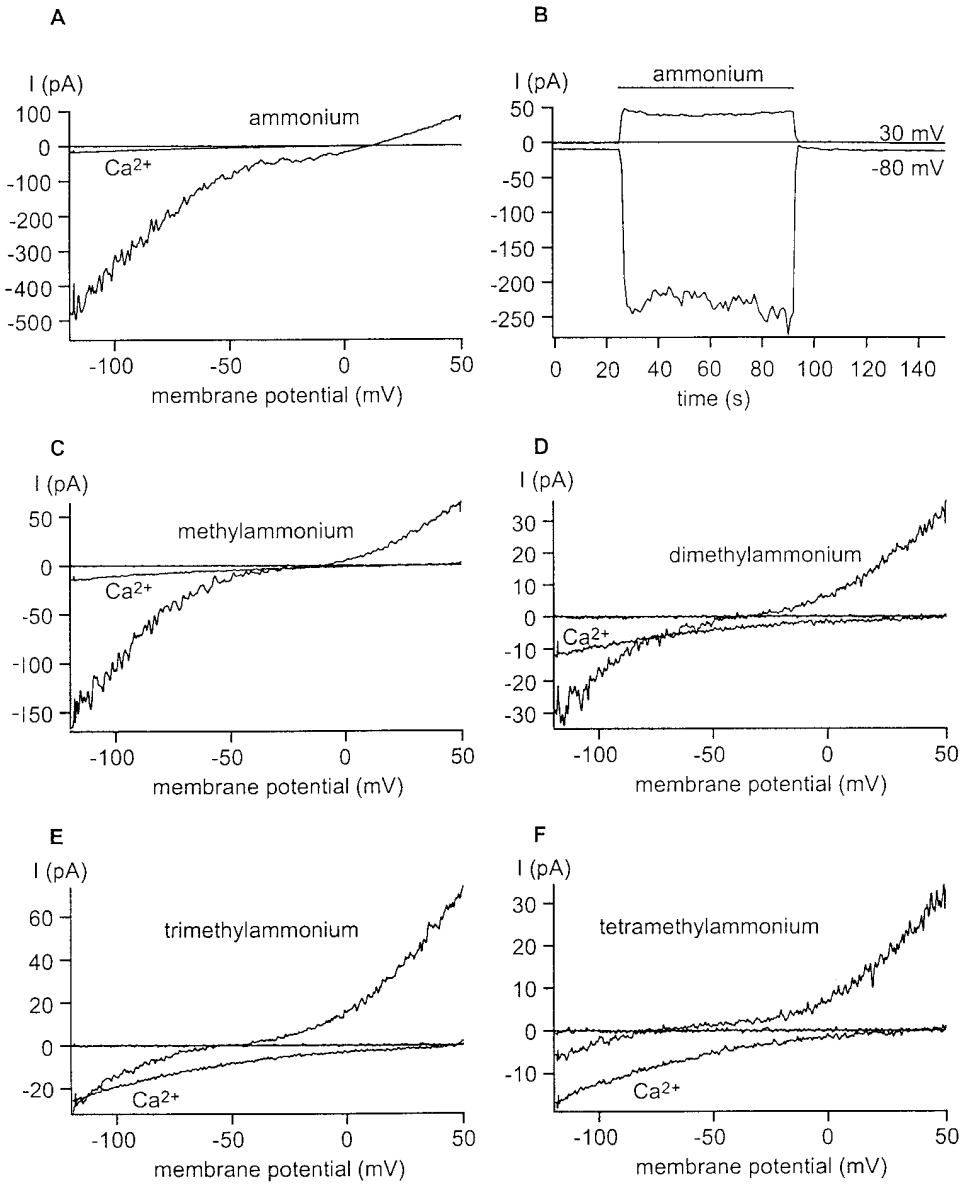

FIGURE 2. Permeability of CRAC channels to organic cations. CRAC channels were activated during whole-cell dialysis with Na^+ aspartate. The external solution contained 1 μM Ca^{2+} and 150 mM X^+, where X^+ is ammonium (*A* and *B*), methylammonium (*C*), dimethylammonium (*D*), trimethylammonium (*E*), tetramethylammonium (*F* and *J*), ethylammonium (*G*), isopropylammonium (*H*), and $NMDG^+$ (*I* and *J*). Most panels illustrate currents using voltage ramps as in Fig. 1; note that the current amplitude scales vary. For these panels, three ramp traces show, including one before activation of CRAC channels, Ca^{2+} currents through CRAC channels with 20 mM $[Ca^{2+}]_o$, and monovalent currents upon lowering $[Ca^{2+}]_o$ to 1 μM. (*B* and *J*) Current amplitudes at −80 and +30 mV before and after changing the bath solution from 20 mM Ca^{2+} to 1 μM Ca^{2+} containing ammonium (*B*) or TMA^+ followed by $NMDG^+$ (*J*). The bars above the current correspond to the main external cation. Note that the NH_4^+ currents are sustained in *B*. In *I* and *J*, there are no detectable inward currents carried by $NMDG^+$. TMA^+ carries a small but detectable inward current (*F* and *J*).

age-gated Ca^{2+} channels. The permeability of CRAC channels to Na^+ and other alkali cations diminishes with time after exposure to low $[Ca^{2+}]_o$. The current carried by Na^+ immediately after lowering $[Ca^{2+}]_o$ is 5- to 10-fold larger than the preceding Ca^{2+} current. Cs^+, although nearly as permeant as Na^+ from reversal potential measurements, carries much less inward current than Na^+. In the following experiments, we compare the reversal potentials, permeabilities relative to Na^+, rectification, and kinetics of the CRAC channel carrying monovalent organic cations.

Permeability of CRAC Channels to Organic Cations

We used a series of organic monovalent cations to obtain further information about the selectivity of CRAC channels and to estimate the minimal cross-sectional diameter of the conducting pore. We substituted the organic cations for Na^+ in the external solution, measured reversal potentials E_X and E_{Na}, and calculated the permeability relative to Na^+ using the following equation:

$$E_X - E_{Na} = RT/F \ln P_X [X]_O / P_{Na} [Na]_o, \qquad (1)$$

where X specifies the ion substituted for Na^+. To test for possible contaminating "leak" currents, control experiments with four of the test cations (NH_4^+, hydrazine, methylammonium, and dimethylammonium) were performed to ensure that the monovalent current is not observed under "nondepleted" conditions before CRAC channels activate. Again, as with Na^+, monovalent current carried by organic cations was measured only if CRAC channels were already open. To establish biionic conditions, we chose Na^+ instead of Cs^+ as the internal cation because it passes through the CRAC channel more readily and is less permeant through K^+ channels than Cs^+. Similar results were obtained using internal Cs^+ (data not shown). Assuming that internal concentrations remain constant when external solutions are exchanged, the permeability ratio P_X/P_{Na} for the test cation relative to Na^+ can be calculated from the change in reversal potential, $E_X - E_{Na}$. Since monovalent ions are only permeant through CRAC channels under conditions of low divalence, we performed all experiments with organic monovalent ions in 1 μM $[Ca^{2+}]_o$.

The organic cations varied substantially in their permeability through CRAC channels. Fig. 2 demonstrates that increasing the number of methyl groups on NH_4^+ shifted the reversal potentials to the left, indicating re-

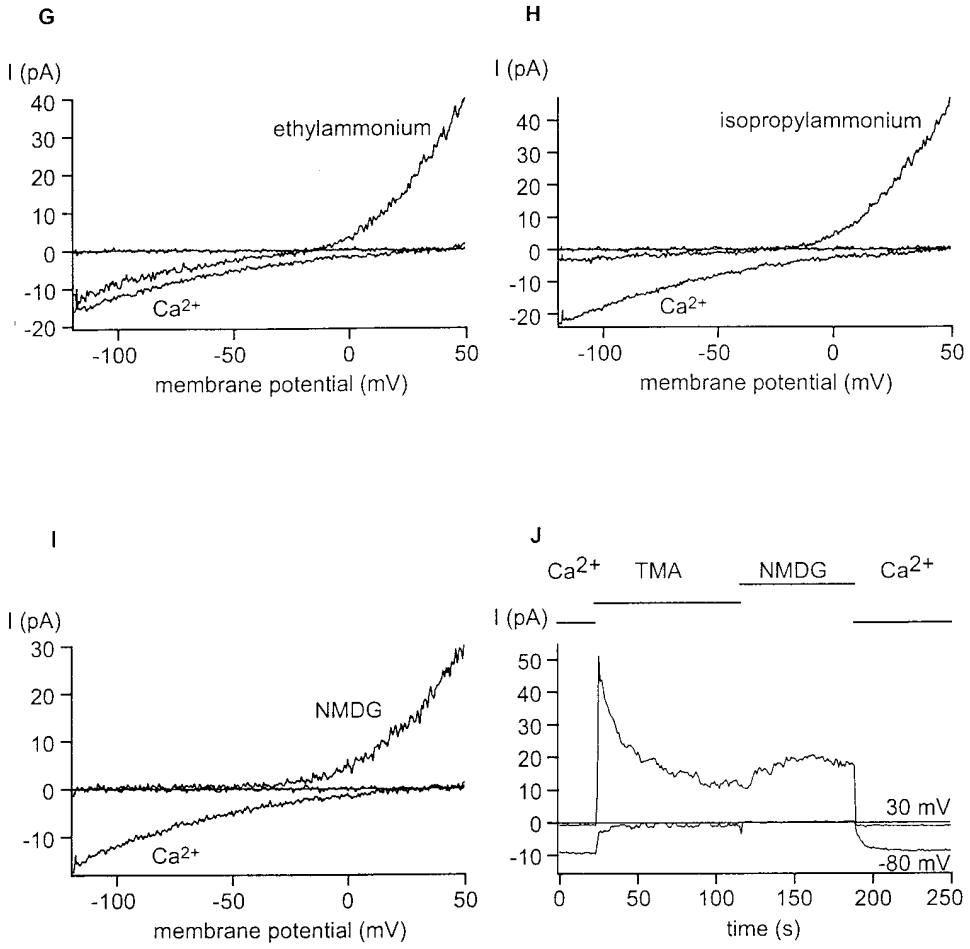

FIGURE 2. (*Continued*)

duced permeability. The most permeant ion tested was NH_4^+ (P_{NH4}/P_{Na} = 1.37; Fig. 2 *A*), and the least measurably permeant ion was TMA^+ (P_{TMA}/P_{Na} = 0.09; Fig. 2 *F*). Ethylammonium (Fig. 2 *G*) and isopropylammonium (Fig. 2 *H*) were more permeant than the symmetrical and bulkier TMA^+ (Fig. 2 *F*). With external $NMDG^+$, inward currents were not measurable (Fig. 2 *I*), suggesting that $NMDG^+$ is not permeant through CRAC channels.

In parallel with the shift of the reversal potential to the left, the magnitude of the inward current decreased. Note that the scales in Fig. 2 vary depending on the cation being tested. Inward ramp currents measured at −80 mV carried by NH_4^+ or TMA^+ differed by a factor of 100. Outward currents carried by Na^+ were less affected. A direct comparison of TMA^+ and $NMDG^+$ is shown in Fig. 2 *J*.

Table I and Fig. 3 summarize reversal potentials and permeability ratios for the organic cations tested. The permeability ratios can be used to estimate the diameter of the selectivity filter. The largest ion used, TMA^+, has a diameter of 0.55 nm, indicating that the cross-sectional diameter of the conducting path through a CRAC channel at its narrowest region is at least this size. We calculated permeability ratios and estimated the size of the selectivity filter, assuming that steric hindrance determined permeability differences but not the electrostatic interaction between ion channel and cation. The ion channel is considered as a water-filled pore, obeying a simple hydrodynamics equation:

$$P_X/P_{Na} = \kappa[1 - (d_{ion}/d_{pore})], \quad (2)$$

where P_X/P_{Na} is the permeability ratio, κ is a proportionality constant, d_{ion} is the diameter of the ion, and d_{pore} is the diameter of the pore (Dwyer et al., 1980; Burnashev et al., 1996). The line drawn in Fig. 3 relates only to the size of the pore but does not include energetic changes associated with the permeation of the ion through the pore. The estimated diameter of the pore is at least 0.58 nm. Although CRAC channels are amazingly selective for Ca^{2+} over monovalent ions in physiologic ion solutions, they become relatively nonselective when $[Ca^{2+}]$ is reduced to micromolar levels, indicative of a rather large pore.

TABLE I

Permeability of Monovalent Cations through CRAC Channels

Ion	E_x	P_x/P_{Na}
	mV	
Na^+	0 ± 3 (n = 10)	—
K^+	0 ± 3 (n = 3)	1.0
Li^+	0 ± 4 (n = 4)	1.0
Cs^+	0 ± 4 (n = 5)	1.0
Ammonium	+8 ± 2 (n = 6)	1.37
Methylammonium	−11 ± 4(n = 9)	0.65
Dimethylammonium	−33 ± 3(n = 9)	0.28
Trimethylammonium	−52 ± 1(n = 3)	0.13
Tetramethylammonium	−62 ± 2 (n = 7)	0.09
Ethylammonium	−15 ± 2 (n = 8)	0.56
Isopropylammonium	−22 ± 1(n = 3)	0.42
Hydrazine	−6 ± 2 (n = 4)	0.79
N-methyl-D-glucamine	<−120 (n = 6)	<0.0085

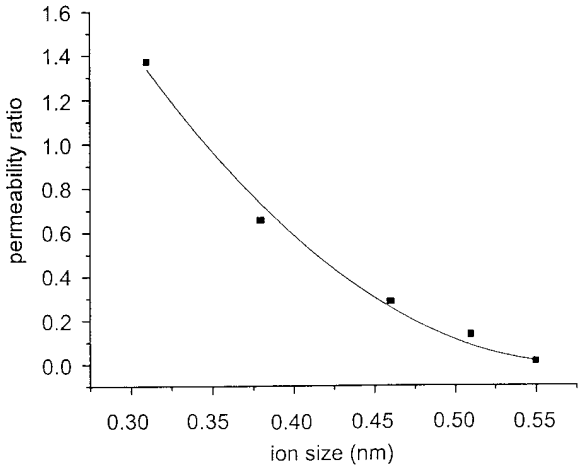

FIGURE 3. Estimation of the pore size of CRAC channels. Permeability ratios P_X/P_{Na} of ammonium and its methylated derivatives were calculated from measured reversal potentials using Eq. 1 and plotted as a function of the geometric mean diameter of the organic cation. The line represents a fit to Eq. 2. The extrapolated diameter of the pore is 0.58 nm.

pH Dependence of Kinetics and Current Magnitude

After the development of I_{CRAC} in 20 mM $[Ca^{2+}]_o$, exposure to 1 μM $[Ca^{2+}]_o$ produced an inward Na^+ current that declined towards zero within several tens of seconds (Fig. 1 *D*). For simplicity, we will refer to this decline of monovalent current as "inactivation." In contrast, with NH_4^+ and related organic cations in the external solution, inward and outward currents through CRAC channels were sustained (Fig. 2 *B*). Ammonium and related cations exist in equilibrium with neutral molecules that may cross the membrane in their uncharged form and subsequently be reprotonated, resulting in alkalinization of the internal solution. Therefore, we investigated the effects of varying internal pH on the kinetics of the Na^+ current upon divalent withdrawal. We controlled intracellular pH (pH_i) by dialyzing the cell with internal solution buffered between pH 6.2 and 8.2. The current time courses and representative I-V curves are illustrated in Fig. 4. Increasing pH_i did indeed reduce the inactivation of Na^+ current through CRAC channels, as predicted from the hypothesis that NH_3 crossing the membrane alkalinized the cy-

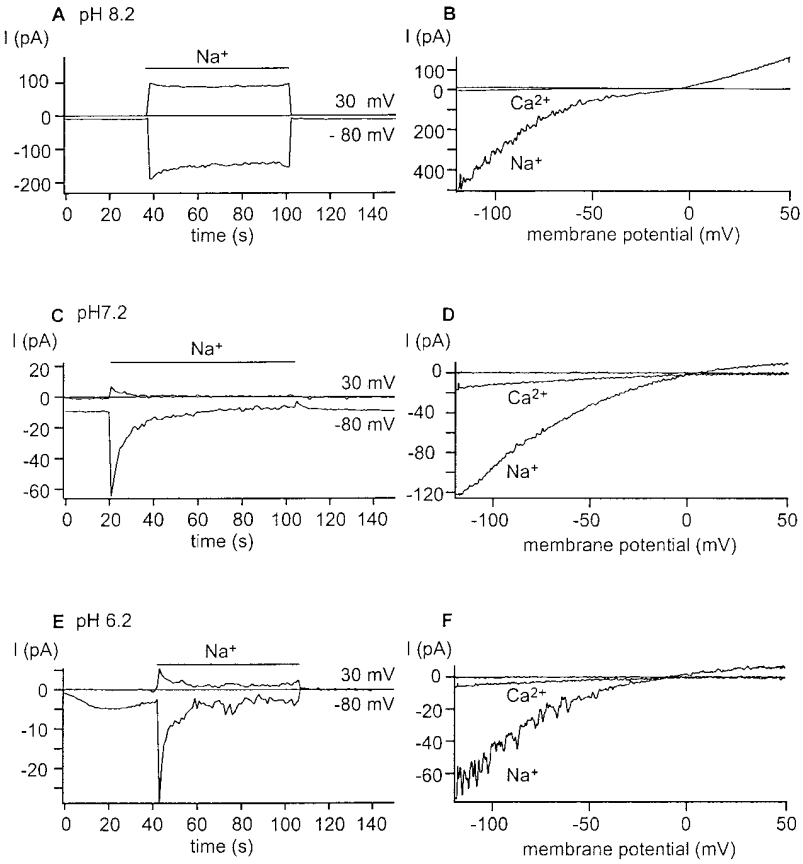

FIGURE 4. Effects of internal pH on current kinetics and magnitudes. CRAC channels were activated during dialysis with Na^+ aspartate pipette solution, titrated to pH 8.2 (*A* and *B*); 7.2 (*C* and *D*), or 6.2 (*E* and *F*). Time courses of currents at −80 and +30 mV are shown on the left, and selected ramp traces illustrating currents carried by Ca^{2+} or Na^+ are shown on the right. Changing the external solution from 20 mM to 1 μM $[Ca^{2+}]_o$ induced inward currents carried by Na^+. Note that the scale for the current varies among the individual figures and that lowering internal pH decreases the current magnitudes and makes the current decline more rapidly. This reduction in current amplitude occurred with either Tris- or HEPES-buffered pipette solution.z

toplasmic side of the membrane (Fig. 4 *A*). Conversely, decreasing pH_i accelerated the rate of decline (Fig. 4 *E*), and also reduced the current amplitude.

To assess the effects of intracellular pH on current amplitude and kinetics, we measured current amplitudes and inactivation rates over a range of pipette pH values, using either HEPES- or Tris-buffered pipette solutions, with identical results. The time course of inactivation upon lowering $[Ca^{2+}]_o$ cannot be fitted well by a single exponential function. For a semi-quantitative index of the inactivation rate, the value of the Na^+ current through CRAC channels 50 s after the maximum activation (I_{50}), relative to the maximum Na^+ current through CRAC channels (I_{max}), was determined and plotted as a function of pH_i in Fig. 5 *A*. This ratio increased from 0.13 ± 0.07 (n = 8) at pH 6.2 to 0.49 ± 0.17 (n = 6) at pH 8.2. We conclude that raising intracellular pH can partially inhibit inactivation with an apparent pK_a value above 8. In addition to the effect on inactivation of monovalent current through CRAC channels, pH_i modulated the magnitude of the current (Fig. 5 *B*). In agreement with the assumption that Na^+ and Ca^{2+} pass through the same CRAC channels, Na^+ and Ca^{2+} current were equally reduced by lowering pH_i. The Ca^{2+} current density was reduced from 1.6 ± 0.2 pA/pF at pH 8.2 (n = 6) to 0.3 ± 0.1 pA/pF at pH 6.2 (n = 10). The pH_i effect on current magnitude was fitted with an apparent pK_a of 6.8 (Fig. 5 *B*). I-V shapes were similar with high and low pH_i. Both pK_a values could be influenced by the fact that true current magnitudes may be underestimated due to rapid compo-

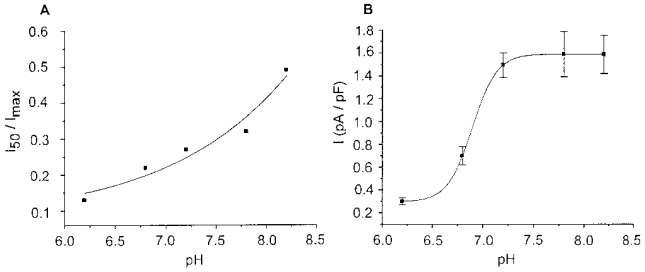

FIGURE 5. pH_i dependence of "inactivation" (*A*) and magnitude (*B*) of Na^+ current through CRAC channels. Solutions as in Fig. 4. (*A*) Na^+ currents at −80 mV through CRAC channels 50 s after lowering $[Ca^{2+}]_o$ (I_{50}) were divided by the maximal Na^+ currents (I_{max}) and plotted as a function of pH_i. The line was drawn to the equation: $I_{50}/I_{max} = b + (1 - b)/[1 + (pH - pK_a)]$, assuming a pK_a of 8.3 and a baseline value b of 0.15. (*B*) Concentration–response relationship for the block of Ca^{2+} current through CRAC channels by internal protons. The line through the points represents a fit to the equation: $I = I_{max}/[1 + (pH - pK_a)]$, with a pK_a of 6.8. Each data point in *A* and *B* represents between 12 and 43 cells.

nents of inactivation that may occur during the solution exchange at low or normal intracellular pH. We conclude that there are at least two distinct sites where intracellular protons modulate the CRAC channel, one favoring inactivation and the other decreasing the magnitude of current through the channel.

Mg^{2+}-dependent Block of CRAC Channels

Both divalent and monovalent currents through CRAC channels exhibit inward rectification. In several other channel types, Mg^{2+} has been shown to block open channels in a voltage-dependent manner and contribute to rectification (Nowak et al., 1984; Vandenberg, 1987; Pusch, 1990; reviewed by Nichols and Lopatin, 1997; Bara et al., 1993). To test whether intracellular Mg^{2+} modulates rectification in CRAC channels, we introduced Mg^{2+}-free internal solution into cells bathed in nominally Ca^{2+}- and Mg^{2+}-free external solution. Large outward currents developed exactly in parallel with inward CRAC currents, as shown in Fig. 6 *A*. Fig. 6 *B* illustrates the I-V shape with very large outward currents that normally are not observed. Although Cs^+ normally conducts poorly through CRAC channels, even when $[Ca^{2+}]_o$ is lowered (e.g., Fig. 1, *A* and *E*), several lines of evidence point to the large outward current being carried by Cs^+ through CRAC channels when cytoplasmic Mg^{2+} is lowered. First, the outward and inward currents activate with the same time course as stores are passively depleted, as illustrated by the scaled records in Fig 6 *A*. Second, in seven experiments with variable current amplitudes, relative current amplitudes at positive and negative potentials were highly consistent (Fig. 6, *legend*), reflecting a consistent I-V shape. If leak currents were responsible for the outward currents, the I-V shapes should vary considerably from cell to cell. Instead, a characteristic sigmoid shape was observed in cells without Mg^{2+} inside, instead of the normal inwardly rectifying I-V observed when Mg^{2+} was present. Third, when $NMDG^+$ was used instead of Cs^+ inside the pipette, the outward currents were much smaller (Fig. 7, *E* and *F*). Fourth, both outward and inward currents were blocked by addition of La^{3+} (300 μM, data not shown). In addition, when Ca^{2+} was included in the external solution, both the inward and outward currents were reduced (see below). These results demonstrate that when Mg^{2+} is excluded from the internal solution, both inward and outward monovalent currents are carried readily through CRAC channels when external Ca^{2+} is lowered. We conclude that internal Mg^{2+} normally blocks outward current through CRAC channels.

In addition to altering I-V characteristics of CRAC channels, removal of internal Mg^{2+} eliminates the slow decline of monovalent current through CRAC channels, a result qualitatively similar to the effect of increasing pH_i. Both inward and outward monovalent currents were sustained upon divalent removal. Similar results were obtained in several experiments with 100 μM $[Mg^{2+}]_i$.

Fig. 7 gives an overview of Ca^{2+}, Na^+, and Cs^+ current through CRAC channels using cells dialyzed with or without internal Mg^{2+}. Recordings from a cell dialyzed with Mg^{2+} (Fig. 7, *A* and *B*) revealed inward currents with magnitudes that varied in the sequence $Na^+ > Ca^{2+} > Cs^+$ at −80 mV. At +30 mV, small outward currents were carried by Cs^+. Despite the huge difference in the magnitude of the inward Na^+ and Cs^+ currents, both had nearly the same reversal potential (Fig. 7 *B*). Thus, with Mg^{2+} inside, Cs^+ carries current poorly, despite being very permeant judging from reversal potentials. However, when Mg^{2+} was excluded from the internal solution, inward and outward current magnitudes were larger, the currents were sustained, and the difference between Na^+ and Cs^+ current magnitudes was erased (Fig. 7, *C* and *D* with Cs^+ aspartate inside, and *E*

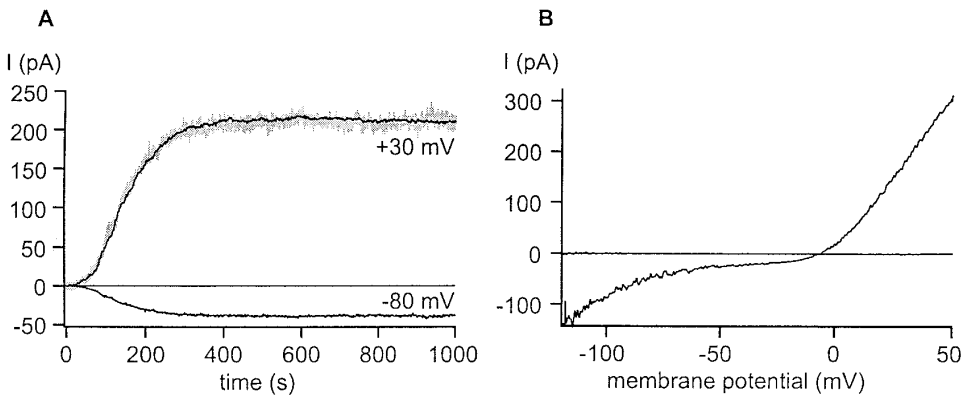

FIGURE 6. Removal of internal Mg^{2+} permits large, sustained inward and outward monovalent currents through CRAC channels. Whole-cell dialysis with Cs^+ aspartate, zero Mg^{2+} pipette solution. The bath contained nominally Ca^{2+}-free external solution. (*A*) Development of outward currents at +30 mV and inward currents at −80 mV. The inward current at −80 mV was inverted, scaled, and superimposed (*light trace*) to the current at +30 mV for comparison. This scaling procedure was done in seven cells, with a consistent scaling factor of 5.9 + 0.3 (mean + S.D.). (*B*) Representative current traces taken from the cell shown in *A* before and activation of CRAC channels with Cs^+ aspartate, 0 Mg^{2+} inside.

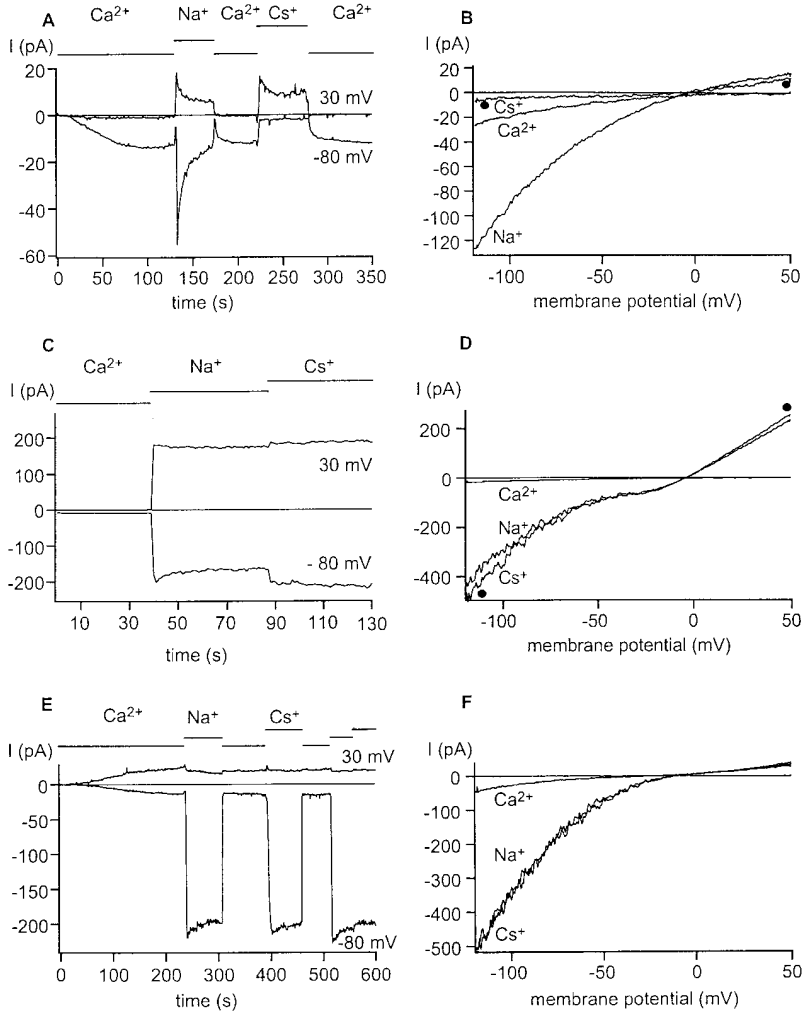

FIGURE 7. Permeability of Na^+ and Cs^+ through CRAC channels with and without internal Mg^{2+}. Ramp currents were recorded every second in 20 mM Ca^{2+} and 1 μM $[Ca^{2+}]_o$ containing either Na^+ or Cs^+ as the main monovalent cation. (*left*) The time course of currents at −80 and +30 mV. The bars above each trace indicate the current carrier. (*right*) Selected I-V ramp currents with Ca^{2+}, Na^+, or Cs^+ carrying current through CRAC channels. Ramp currents with external Cs^+ are marked for identification with •. (*A*) Cs^+ aspartate internal solution containing Mg^{2+}. Note that the Na^+ current declines, as in Fig. 1. When the monovalent current is revealed upon lowering $[Ca^{2+}]_o$, it begins to inactivate with complex kinetics; the inactivation process may begin even before the full Na^+ current can be seen. Thus, the full magnitude of the Na^+ current may not be observed when inactivation is present. Na^+ currents were 5–10-fold larger than the Ca^{2+} current in this series of experiments. (*B*) Representative ramp current traces from the cell shown in *A*. Although Na^+ currents are larger than Cs^+ currents through CRAC channels, both have the same reversal potential. (*C* and *D*) Mg^{2+}-free Cs^+ aspartate internal solution. Lowering $[Ca^{2+}]_o$ unmasks large inward and outward currents that are sustained. Cs^+ and Na^+ currents are comparable in magnitude and in reversal potential. The amplitude of monovalent currents was ~25× larger than the immediately preceding Ca^{2+} current with Mg^{2+} removed (note differences in amplitude scales in *A* vs. *C* and *E*). (*E* and *F*) Mg^{2+}-free $NMDG^+$ aspartate internal solution. Again, Na^+ and Cs^+ inward currents are sustained and similar in magnitude, as well as reversal potential.

and *F* with $NMDG^+$ aspartate inside). The inward current magnitudes varied in the sequence $Na^+ = Cs^+ > Ca^{2+}$. We conclude that internal Mg^{2+} affects channel rectification and the relative ease with which Cs^+ and Na^+ carry current through the CRAC channel. These results can be qualitatively explained by competition between Mg^{2+} bound to the channel and Na^+ moving inward, with Na^+ having a greater ability than Cs^+ to clear the channel of bound Mg^{2+}, resulting in large Na^+ currents but small Cs^+ currents when Mg^{2+} is present. Upon removal of internal and external divalents, Na^+ and Cs^+ carry current equally well.

Fig. 8 provides evidence that internal Mg^{2+} also affects the I-V shape of Ca^{2+} current through CRAC channels. With Mg^{2+} inside, Ca^{2+} current through CRAC channels rectifies inwardly (Fig. 8 *A*). Perfusion of the cell with Mg^{2+}-free internal solution results in a more linear I-V curve through CRAC channels (Figs. 1 and 8 *B*).

Mg^{2+} removal from the inside permits large outward

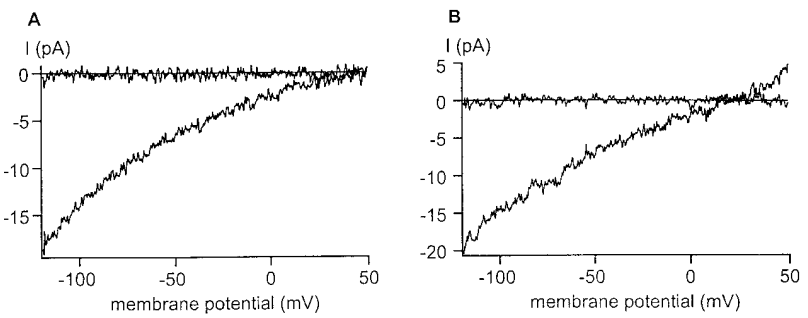

FIGURE 8. Internal Mg^{2+} causes inward rectification of Ca^{2+} current through CRAC channels. (*A*) Cell dialyzed with Cs^+ aspartate, Mg^{2+}-containing solution showing inward rectification. (*B*) Cell dialyzed with Cs^+ aspartate, Mg^{2+}-free internal solution. Current–voltage relation is more linear.

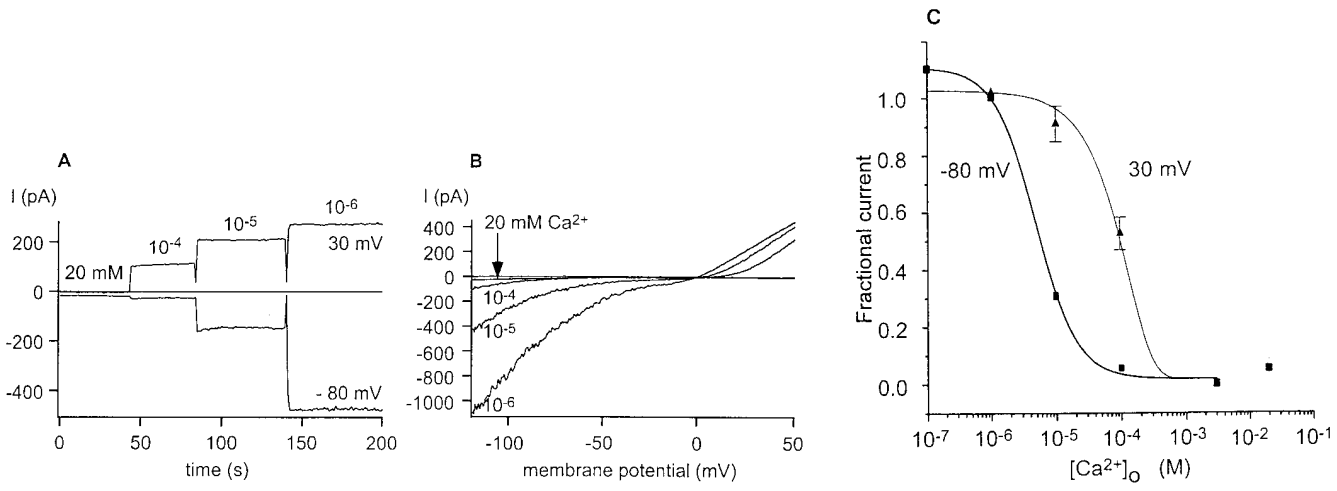

FIGURE 9. $[Ca^{2+}]_o$ blocks Na^+ current through CRAC channels. Cell was dialyzed with Mg^{2+}-free solution containing Cs^+ aspartate, and superfused with external solutions varying in their Ca^{2+} concentration from 2 mM to 0.1 μM. (*A*) Time course of current magnitudes at −80 and +30 mV. (*B*) Ramp currents were taken from the cell shown in *A* and representative current traces in 20 mM $[Ca^{2+}]_o$ before and after activation, and in 100, 10, and 1 μM $[Ca^{2+}]_o$. Note changes in I-V shape; inward currents are reduced to a greater extent than outward currents when the $[Ca^{2+}]_o$ is increased from 1 to 10, and then to 100 μM. With 20 mM $[Ca^{2+}]_o$, Ca^{2+} carries a small inward current and no outward currents is observed. At micromolar levels of $[Ca^{2+}]_o$, inward currents are carried by Na^+; outward currents by Cs^+. (*C*) Concentration-dependent block of Na^+ current through CRAC channels by $[Ca^{2+}]_o$. Current magnitudes at −80 and +30 mV were normalized to values at 1 μM $[Ca^{2+}]_o$ and fitted by the equation $fractional\ I = 1/[1 + ([Ca^{2+}]_o/K_d)]$. Ca^{2+} blocks the Na^+ current through CRAC channels with a K_d of 5 μM at −80 mV and with a K_d of 100 μM at +30 mV. Data from three to six cells are summarized in each data point.

as well as inward monovalent currents, thus enabling the block of monovalent currents by Ca^{2+} to be evaluated at positive as well as negative membrane potentials (Fig. 9). At the beginning of the recording, the cell was superfused with 20 mM Ca^{2+}. Under this condition, only an inward Ca^{2+} current was detectable. Decreasing the external Ca^{2+} concentration to 100 μM revealed an inward current at −80 mV and an outward current at +30 mV. Decreasing $[Ca^{2+}]_o$ further increased both inward and outward currents. Current magnitudes were normalized to the maximum current at or below 1 μM $[Ca^{2+}]_o$, and fitted to a simple equation based upon the assumption that binding of a single Ca^{2+} blocks inward Na^+ current. At −80 mV the K_d value was 5 μM, while at +30 mV the K_d was 100 μM. The results suggest that the apparent K_d may be influenced by the distance that a Ca^{2+} ion must travel to bind to its site within the membrane (Woodhull, 1973).

When $[Mg^{2+}]_i$ or $[Ca^{2+}]_o$ were varied, corresponding I-V shapes suggested voltage-dependent block of monovalent current through CRAC channels by divalent ions. Mg^{2+} preferentially blocks outward current from the inside (Fig. 7, *A* and *D*), and Ca^{2+} preferentially blocks inward current from the outside (Fig. 9 *B*). Assuming that Ca^{2+} or Mg^{2+} may block in a voltage-dependent manner from the outside and inside, respectively, the voltage dependence of block can be assessed by dividing monovalent ramp currents in pairs of cells with or without the divalent blocking ion. To assess the steepness of block, I-V ratios were fitted to a Boltzmann distribution,

$$I_X/I = A/\{1 + \exp[(E_h - E)/k]\}, \qquad (3)$$

where I_X is the current with internal Mg^{2+} or external Ca^{2+} relative to the unblocked current I in the absence of divalents, A is the maximum current ratio, E_h is the voltage at which half of the channels are blocked, and k is the steepness of the block. Fig. 10 *A* shows an example of an I-V ratio, illustrating Mg^{2+} block from the inside. Mg^{2+} induced inward rectification by blocking outward currents at positive potentials. The steepness factor k was −13.3 ± 1.5 mV ($n = 3$), suggesting the existence of a Mg^{2+} binding site within the membrane electric field. In a simple blocking model, the factor k is equivalent to RT/zδF, where R, T, and F have their usual meanings, z is the charge of the blocking ion, and δ is the fractional distance across the electric field that the ion would travel to reach its binding site (Woodhull, 1973). The mean zδ product for Mg^{2+} block of 1.88 would correspond to a single Mg^{2+} ion moving across 94% of the membrane electric field from the inside, or half this distance if two Mg^{2+} ions move.

To analyze the voltage dependence of external Ca^{2+} block, we calculated ratios of I-V curves when $[Ca^{2+}]_o$ was varied from 1 to 100 μM (Fig. 10 *B*). The steepness factor k was 15.4 ± 0.9 mV ($n = 5$), corresponding to a mean zδ product of 1.62 and an "equivalent electrical

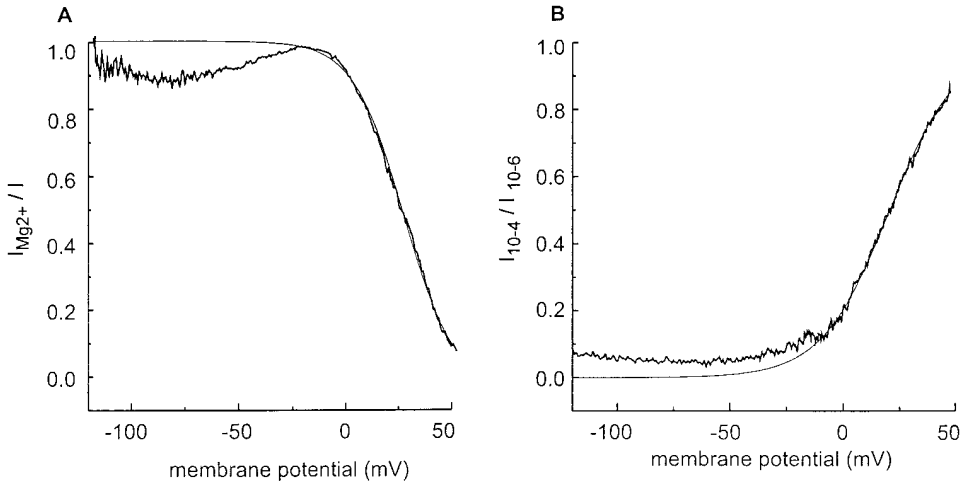

FIGURE 10. Voltage-dependent block by internal Mg^{2+} and external Ca^{2+}. (*A*) Voltage dependence induced by internal Mg^{2+}. Solutions as in Fig. 7; pipette solutions contained Cs^+ aspartate with or without Mg^{2+}. Ramp I-V trace recorded in the presence of internal Mg^{2+} was divided point by point by an I-V trace obtained in a different cell in the absence of internal Mg^{2+}. The smooth line represents a fit to the Boltzmann distribution (Eq. 3). E_h = 20 mV; $k = -13$ mV. (*B*) Voltage dependence of Ca^{2+} block. I-V curves with 100 μM $[Ca^{2+}]_o$ were divided by I-V curves with 1 μM $[Ca^{2+}]_o$ and fitted to a Boltzmann relation. E_h = 20 mV; k = 15 mV.

distance" of 81% across the membrane electric field from the outside. Thus, both Mg^{2+} from the inside and Ca^{2+} from the outside block monovalent current through CRAC channels in a steeply voltage-dependent manner.

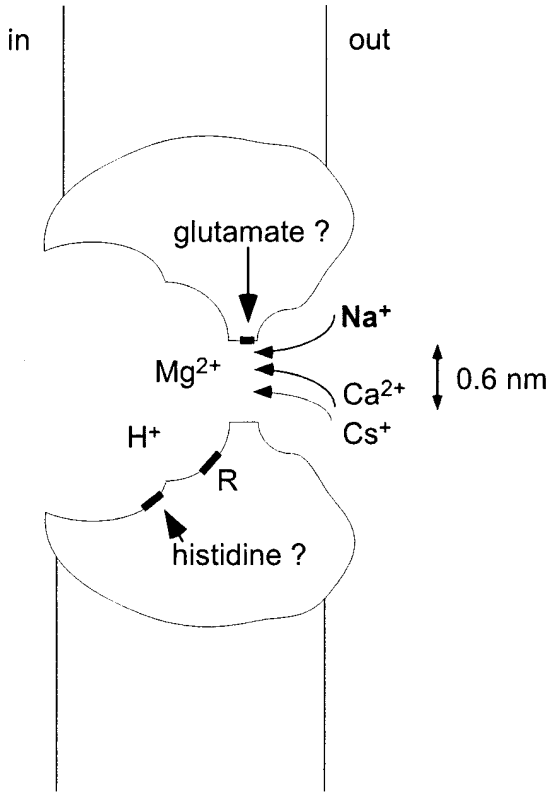

FIGURE 11. A cartoon view of three sites and ionic interactions in the CRAC channel. We assume that glutamate residues at the selectivity filter are important for ion permeation, in analogy with results from voltage-gated Ca^{2+} channels (Ellinor et al., 1995). The glutamate residues surround the narrowest region of the pore 0.6 nm in diameter. Ca^{2+} and Na^+ are shown as they encounter the selectivity filter from the outside; a frustrated Cs^+ cannot pass through because of Mg^{2+} bound to the site within the pore. A separate site shown as a histidine (pK_a of 6.8) is shown facing the cytoplasm where it regulates conductance. A basic amino acid residue R ($pK_a > 8$) regulates inactivation.

DISCUSSION

We first present a cartoon to illustrate several properties of CRAC channels described in this paper. Fig. 11 depicts three distinct sites, including a selectivity filter, a site facing the cytoplasm that regulates conduction, and a basic residue that regulates inactivation. In addition, Ca^{2+}, Mg^{2+}, Na^+, Cs^+, and H^+ ions are shown as they interact with these sites.

Our experiments demonstrate that CRAC channels carry large and sustained inward and outward monovalent currents when internal and external divalent ion concentrations are reduced to the micromolar level. In the absence of external divalents, the CRAC channel displays a large, weakly selective pore that discriminates among organic cations by molecular sieving. Internal Mg^{2+} appears to exert three effects upon the CRAC channel. First, Mg^{2+} as an internal voltage-dependent blocking ion, sculpts the I-V relationship by preferentially reducing the outward current, thereby inducing inward rectification. Second, Mg^{2+} modulates the relative currents carried by different monovalent cations, perhaps by competing with specific monovalent ions, making the current for Cs^+ small compared with that for Na^+. Third, Mg^{2+} is required for inactivation of monovalent current upon lowering $[Ca^{2+}]_o$. Raising pH_i exerts effects similar to the removal of internal Mg^{2+}, whereas reducing pH_i inhibits divalent or monovalent current through the CRAC channel. External Ca^{2+} regu-

lates channel selectivity by selective binding. As $[Ca^{2+}]_o$ is raised in the micromolar range, monovalent currents are reduced as Ca^{2+} blocks in a voltage-dependent manner within the pore. As $[Ca^{2+}]_o$ is raised further into the millimolar range, Ca^{2+} moves selectively across the channel, but Ca^{2+} currents are small compared with the monovalent currents.

Sizing the CRAC Channel

What is the minimal size of the conducting pore? To obtain an estimate, we reduced extracellular $[Ca^{2+}]$ to permit monovalent conduction and measured reversal potentials using a series of nine organic compounds as probes of varying size (Figs. 1 and 2; Table I). Our results show that ammonium derivatives exhibit a well-ordered permeability sequence depending upon ionic size, ranging from NH_4^+ with $P_{NH4}/P_{Na} = 1.37$ to TMA^+ with $P_{TMA}/P_{Na} = 0.09$. The largest permeant cation used, TMA^+, has a diameter of 0.55 nm, indicating that the pore of the CRAC channel is at least this size. Assuming only volume exclusion, and neglecting the friction between the ion channel and the organic cation and the viscosity of the medium surrounding the ion (Dwyer et al., 1980), the extrapolated diameter of the pore is 0.58 nm (Fig. 3). We attempted to measure current with $NMDG^+$, an asymmetric molecule with a minimal cross-section corresponding to 0.5×0.64 nm. With external $NMDG^+$, inward currents were not detected above -120 mV, placing the value of $P_{NMDG}/P_{Na} < 0.0085$. Although highly selective for Ca^{2+} and with an extremely small unitary conductance, the CRAC channel pore is physically large enough to accommodate molecules up to roughly 0.6 nm in diameter.

Inactivation of Monovalent Current

What type of process accounts for the decline (inactivation) of monovalent current after removal of extracellular Ca^{2+}? Our results indicate that both protons and Mg^{2+} ions in the cytoplasm are required (Figs. 4–7). In low Ca^{2+} Ringer, the Na^+ current through CRAC channels is transient, gradually declining over tens of seconds with at least two exponential components. For simplicity, but without mechanistic implication, we refer to the decline of monovalent current as "inactivation." After inactivation and upon readdition of extracellular Ca^{2+}, the Ca^{2+} current increases with complex kinetics, including a very rapid initial phase followed by a slower increase that has been termed "Ca^{2+}-dependent potentiation" (Zweifach and Lewis, 1996). In the course of examining the permeability of the channel to organic cations, we noticed that inactivation was greatly reduced when NH_4^+ was substituted for Na^+. We hypothesized that movement of neutral NH_3 across the membrane might raise the cytoplasmic pH, despite the presence of intracellular buffer, and that alkalinization of the cytoplasm near the CRAC channel could prevent inactivation. Consistent with this hypothesis, we found that raising internal pH by dialysis of pH-buffered solutions reduced the extent of inactivation; the pKa for this kinetic effect is above 8 (Figs. 4 and 5).

In addition, we found that the inactivation process requires internal Mg^{2+} (Figs. 6 and 7). With internal Mg^{2+} reduced to 100 μM or lower, monovalent currents were sustained, regardless of the current carrier or the direction of current flow. Inactivation and the reverse process of Ca^{2+}-dependent potentiation may be due to the binding and unbinding, respectively, of Mg^{2+} ions to a site or sites associated with the CRAC channel. Let us assume that the binding site for Mg^{2+} is located at a selectivity filter region near the external membrane surface, consistent with strong voltage-dependent block shown in Fig. 10. Upon readdition, Ca^{2+} would have to compete with Mg^{2+} to pass through the channel. This competition may be reflected in the time course of calcium-dependent potentiation (see Figs. 1, 4, and 7 *A*). External Ni^{2+} can substitute for Ca^{2+} in mediating potentiation (see Fig. 9 in Zweifach and Lewis, 1996). Ni^{2+} may bind with low affinity to the same binding site as Mg^{2+}, dislodging Mg^{2+} but allowing Ca^{2+} to carry current immediately. At depolarized potentials, Mg^{2+} binds more strongly, consistent with the reduced extent of calcium-dependent potentiation at depolarized potentials (see Fig. 4 in Zweifach and Lewis, 1996). To summarize, Ca^{2+}-dependent potentiation may arise from competition between internal Mg^{2+} and external Ca^{2+} for a site near the outer membrane surface.

Mechanism of Inward Rectification and Block by Divalents

What controls inward rectification of Ca^{2+} and monovalent current through CRAC channels? Is it an intrinsic property of the conducting pore, or do blocking ions contribute? There is ample precedent for Mg^{2+} ions playing a role in rectification of other channels. For example, cytoplasmic Mg^{2+} causes fast voltage-dependent block in inward rectifying K^+ and Na^+ channels (Vandenberg, 1987; Pusch, 1990). Inward rectification through CRAC channels is observed whether the inward current is carried by Ca^{2+} or by Na^+. Our results indicate that internal Mg^{2+} blocks outward current through CRAC channels. Removal of Mg^{2+} ions from the pipette solution resulted in much larger outward monovalent currents through CRAC channels, consistent with a voltage-dependent Mg^{2+} block mechanism for rectification. In the simplest model for voltage-dependent block (Woodhull, 1973), an ion is attracted towards or repelled from a site within the membrane according to the electric field. By fitting a Boltzmann relation to ratios of the I-V relations with and without internal Mg^{2+}, we identify a putative Mg^{2+}-binding site

within the membrane. The steepness of block ($z\delta$ = 1.88) would be equivalent to one Mg^{2+} moving almost completely across the membrane from the inside (Fig. 10 *A*).

Ca^{2+} blocks the monovalent current through CRAC channels at an externally accessible site, with affinity in the micromolar range (Figs. 9 and 10). With the inactivation process and block of outward currents eliminated by removal of internal Mg^{2+}, we examined the voltage dependence of Ca^{2+} block over a wide range of potentials and found that the apparent affinity is reduced at positive potentials. At −80 mV, Ca^{2+} blocks the inward current with a K_d of 5 μM, but at +30 mV the K_d was 100 μM. Our K_d value of 5 μM at −80 mV (internal Mg^{2+} removed) is in excellent agreement with the K_d value for Ca^{2+} block determined previously (4 μM at −80 mV, with internal Mg^{2+} present; Lepple-Wienhues and Cahalan, 1996), suggesting that internal Mg^{2+} does not alter the affinity of external Ca^{2+} for the blocking site within the channel. To examine the voltage dependence of Ca^{2+} block in greater detail, we analyzed I-V shapes at varying $[Ca^{2+}]_o$ levels in the absence of internal Mg^{2+}. Block by external Ca^{2+} is steeply voltage dependent ($z\delta$ = 1.62), corresponding to an externally accessible site located at an equivalent electrical distance of 81% across the membrane from the outside.

Both Mg^{2+} block from the inside and Ca^{2+} block from the outside are steeply voltage dependent. The steepness of block suggests movement of a divalent ion most of the way across the membrane to a blocking site. How can we reconcile the existence of steeply voltage-dependent block by internal Mg^{2+} and external Ca^{2+}? Are there two distinct sites on opposite sides of the membrane electric field where divalent ions can bind? Alternatively, the voltage dependence would also be compatible with a single site or sites (the selectivity filter?) located midway through the channel that can attract two divalent ions, with Mg^{2+} or Ca^{2+} able to bind to this site, gaining access from opposite sides of the membrane. Finally, we cannot yet be certain whether the internally accessible Mg^{2+} binding site(s) controlling rectification, relative Cs^+ conductance, and inactivation are one and the same. It is uncertain whether a Mg^{2+} ion can function as the inactivation gate or instead alters the access to an inactivated conformation of the protein.

Permeation Properties of CRAC and Voltage-gated Ca^{2+} Channels

Our data permit a detailed comparison of ion permeation in two very different types of Ca^{2+}-selective ion channels, as summarized in Table II. Although entirely different gating mechanisms are responsible for channel activation (depolarization vs. depletion of intracellular Ca^{2+} stores), several similarities and some interesting differences exist. Upon reducing $[Ca^{2+}]_o$ to micromolar levels, voltage-gated Ca^{2+} channels in various

TABLE II

Ion Permeation in Voltage-gated Ca^{2+} and CRAC Channels

Property	Voltage-gated	CRAC
Ca^{2+} dependence of current	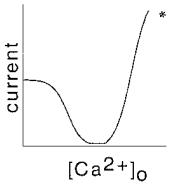	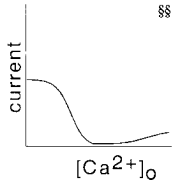
K_d ($Ca^{2+}{}_o$ block)	0.7 μM*	4; 5 μM§§
Voltage dependence of K_d	Increases at negative E‡‡	Decreases at negative *E*
Unitary Ca^{2+} conductance	8 pS§	24 fS***
Unitary Na^+ conductance	85 pS§	2.6 pS§§
Monovalent conductance sequence	$Na^+ > Li^+$§	$Na^+ > Li^+ = K^+ > Rb^+ >> Cs^+$§§
Monovalent permeability sequence	$Li^+ > Na^+ > K^+ > Cs^+$§	$Na^+ \approx Li^+ \approx K^+ \approx Cs^+$
Divalent conductance sequence	$Ba^{2+} > Ca^{2+} \approx Sr^{2+}$§	$Ca^{2+} > Ba^{2+} \approx Sr^{2+} >> Mn^{2+}$‖
Divalent permeability sequence	$Ca^{2+} > Sr^{2+} > Ba^{2+} >> Mg^{2+}$§	?
Conductance sequence affected by $Mg2^+{}_i$	?	Yes, $Na^+ \approx Cs^+$
Rectification affected by $Mg^{2+}{}_i$	Yes, inward rectification**	Yes, inward rectification
Pore size	0.6 nm¶¶	0.6 nm
pK_a (external pH block)	8.5‡	8.2‖‖
PK_a (internal pH block)	6.6¶	6.8

*Almers and McCleskey, 1984; ‡Chen et al., 1996; §Hess et al., 1986; ‖Hoth and Penner, 1993; ¶Kaibara and Kameyama, 1988; **Kuo and Hess, 1993; ‡‡Lansman et al., 1986; §§Lepple-Wienhues and Cahalan, 1996; ‖‖Malayev and Nelson, 1995; ¶¶McCleskey and Almers, 1985; ***Zweifach and Lewis, 1993.

preparations become permeable to monovalent cations, exhibiting only weak selectivity among alkali metal ions (Kostyuk and Krishtal, 1977; Kostyuk et al., 1983; Almers et al., 1984; Almers and McCleskey, 1984; Hess et al., 1986). CRAC channels characterized in lymphocytes and mast cells are voltage independent and highly selective for Ca^{2+} against monovalent ions when both are present (Lewis and Cahalan, 1989; Hoth and Penner, 1993; Zweifach and Lewis, 1993). However, reducing Ca^{2+} and Mg^{2+} in the extracellular solution allows alkali metal cations to pass through CRAC channels (Hoth and Penner, 1993; Lepple-Wienhues and Cahalan, 1996). Below, we compare the following features of ion permeation in voltage-gated Ca^{2+} and CRAC channels: the Ca^{2+} dependence of selectivity and current magnitudes, conductance and permeability sequences, I-V rectification and block by internal Mg^{2+}, the physical size of the conducting pore, and block by internal H^+.

Selectivity and Current Magnitudes are Controlled by External Ca^{2+}

The remarkable Ca^{2+} selectivity of voltage gated Ca^{2+} channels is achieved by selective binding of Ca^{2+} to the ion channel (Almers and McCleskey, 1984; Hess and Tsien, 1984). With $[Ca^{2+}]_o$ in the micromolar range, Ca^{2+} acts as a blocking ion, reducing the nonselective monovalent current with a K_d of ~1 μM, similar to the Ca^{2+}-dependent block of CRAC channels at −80 mV, with a K_d of 4 μM (Lepple-Wienhues and Cahalan, 1996) and 5 μM (present study). Therefore, the ability of voltage-gated Ca^{2+} channels and CRAC channels to exclude monovalent cations depends on the binding of Ca^{2+} to a high affinity site(s). At higher $[Ca^{2+}]_o$ concentrations, Ca^{2+} current can be measured, and a difference between CRAC and voltage-gated Ca^{2+} channels is revealed. The relationship between current and $[Ca^{2+}]_o$ rises less steeply for the CRAC channel. The small size of the Ca^{2+} current, relative to large monovalent current amplitudes, is a characteristic feature of the CRAC channel. Normally, if Mg^{2+} is included in the pipette solution, the peak Na^+ current immediately after lowering $[Ca^{2+}]_o$ compared with the immediately preceding Ca^{2+} current at −80 mV, is 5- to 10-fold larger (Lepple-Weinhues and Cahalan, 1996). In the present experiments when internal Mg^{2+} was present, we found an average ratio of Na^+ to Ca^{2+} current of 7.5 ± 2.7 (mean ± SD; $n = 7$). In experiments with reduced internal Mg^{2+}, the ratio between Na^+ and Ca^{2+} current magnitudes averaged 24.6 ± 4.9 ($n = 6$). We believe that the latter value more accurately reflects the relative ability of the CRAC channel to carry Na^+ versus Ca^{2+}, because some inactivation may occur before a complete solution exchange in experiments with internal Mg^{2+}. The ratio of monovalent current at low $[Ca^{2+}]_o$ to Ca^{2+} current at high $[Ca^{2+}]_o$ is reflected in the shape of the relationship between current and $[Ca^{2+}]_o$, as Table II illustrates diagrammatically. With $[Ca^{2+}]_o$ in the micromolar range, the K_d values for block of monovalent current are very similar, suggesting a site with a similar energy well for both channels. However, as $[Ca^{2+}]_o$ is elevated and Ca^{2+} ions begin to carry significant current, current increases much more steeply for voltage-gated than for CRAC channels.

Under similar ionic conditions, the single-channel conductance of L-type voltage-gated Ca^{2+} channels is 300× larger than that of CRAC channels. The relative ease with which Ca^{2+} moves through the voltage-gated Ca^{2+} channel may also account for the difference in voltage dependence for Ca^{2+} block. In the voltage-gated Ca^{2+} channel, hyperpolarization increases the K_d for Ca^{2+} block, perhaps because Ca^{2+} has a greater tendency to go through the channel rather than simply blocking at negative potentials (Lansman et al., 1986). In CRAC channels, the K_d for Ca^{2+} block decreases as the membrane potential is made more negative, as one would expect for simple voltage-dependent block, perhaps also a consequence of a higher barrier for movement through the membrane.

The ability of voltage-gated Ca^{2+} channels to carry Ca^{2+} current is thought to involve interactions between two or more Ca^{2+} ions inside the channel. Early energy barrier models for Ca^{2+} channel permeation depicted two distinct sites with repulsion between bound Ca^{2+} ions (Hess and Tsien 1984; Almers and McCleskey, 1984). Recent molecular evidence favors a single site consisting of a ring of glutamates contributed by each of four Ca^{2+} channel domains (Ellinor et al., 1995). The Ca^{2+} binding affinity of the glutamate ring may be altered by an approaching Ca^{2+} ion, as proposed before molecular identification of the site (Armstrong and Neyton, 1991). Regardless of mechanistic details, interactions between Ca^{2+} ions would facilitate Ca^{2+} influx. We propose that a similar mechanism operates in CRAC channels, but that the repulsive interaction between Ca^{2+} ions is reduced, or that the overall energy barrier is higher than in the voltage-gated Ca^{2+} channel. This would account for the shallower I-$[Ca^{2+}]_o$ relation, the lower single channel conductance, and the difference in voltage dependence for Ca^{2+} block in CRAC channels.

Conductance and Permeability Sequences

As summarized in Table II, CRAC channels under low divalent conditions exhibit differences in permeability sequences (defined from reversal potentials) and conductance sequences (from current magnitudes) among the alkali metal ions Na^+, K^+, Li^+, and Cs^+. In addition, the conductance sequence and rectification of the CRAC channel can be modulated by internal Mg^{2+} (Fig. 7). Cs^+ represents the clearest anomaly. Although

highly permeant based upon reversal potential measurements, Cs^+ carries inward current very poorly with internal Mg^{2+} present. In terms of Eyring rate theory and simple barrier models for permeation, this difference can be accounted for by Cs^+ ions having a deeper energy well to traverse, but similar energy barriers, relative to Na^+. In other words, Cs^+ may bind more tightly to a site within the channel, resulting in smaller current magnitudes. In contrast, with Mg^{2+} removed, Cs^+ and Na^+ were equally effective in carrying inward current. We envision a competitive interaction between Mg^{2+} bound at or near the selectivity filter and Na^+ as it approaches the site from the outside. In this view, Na^+, but not Cs^+, would be able to compete with Mg^{2+} and move through the channel. An alternative view would be that Mg^{2+} binding allosterically affects the relative Na^+ and Cs^+ affinities, making Cs^+ sticky by lowering an energy well. These proposals are amenable to further experimental tests. Mg^{2+} does not carry appreciable currents through the CRAC channel; for now we assume that it cannot go through, although its presence inside the channel can regulate the relative ability of Cs^+ to carry inward current compared with Na^+.

Rectification and Block by Internal Mg^{2+}

Internal Mg^{2+} blocks Ca^{2+} and monovalent Na^+ and Li^+ current through voltage-gated Ca^{2+} channels (Agus and Morad, 1991; Kuo and Hess, 1993). Block of the monovalent current is strongly voltage dependent, resulting in inward rectification (Kuo and Hess, 1993). To account for the strong voltage dependence of the on-rate (e-fold increase per ~15 mV), a high affinity binding site for Mg^{2+} close to the external mouth of the pore was proposed (Kuo and Hess, 1993). Internal Mg^{2+} is responsible for inward rectification of CRAC channels, with an e-fold increase in block per 13 mV also suggesting a binding site close to the outside. Therefore, CRAC and voltage-gated Ca^{2+} channels may exhibit a similar energy profile for Mg^{2+} block inside the pore.

Pore Size

When probed with organic cations of varying size, both voltage-gated and CRAC channels are revealed to be large, nonselective cation pores of ~0.6 nm in dimension. Even TMA^+ can be accommodated and carries a measurable current in both channels. Unitary Ca^{2+} currents of voltage-gated Ca^{2+} channels are estimated to be 300-fold larger than in CRAC channels, despite the similarity in pore dimension. Ca^{2+} and Na^+ have ionic radii of 0.099 and 0.095 nm, respectively. Unlike the molecular sieving of organic compounds with varying size, selectivity between Ca^{2+} and Na^+ must arise as a result of interactions between the ion, the channel, and water molecules. Ca^{2+} (normally) or Na^+ (if $[Ca^{2+}]_o$ is low) would be able to permeate with at least one associated water molecule, and multiple ions would be able to fit into the large selectivity filter region.

Modulation by pH

CRAC channels and voltage gated Ca^{2+} channels have similar sensitivities to external and internal pH, as summarized in Table II. Our data indicate that pH_i modulates current magnitudes through CRAC channels, as well as the rate of inactivation. Current magnitudes for both Ca^{2+} and monovalent currents are reduced as pH_i is lowered, with a pK_a of 6.8 suggesting a histidine; no voltage dependence was observed. Reducing pH_i has been reported to reduce Ca^{2+} current through voltage-gated Ca^{2+} channels with a similar pK_a (Kaibara and Kameyama, 1988; Klöckner and Isenberg, 1994). The rate of CRAC channel inactivation of monovalent current was accelerated by lowering pH_i, with a pK_a of >8, suggesting a separate site of action. External pH has previously been shown to alter current magnitudes in both CRAC and voltage-gated Ca^{2+} channels. Malayev and Nelson (1995) reported that raising extracellular pH increases the magnitude of CRAC channels in macrophages with a pK_a of 8.2. In voltage-gated Ca^{2+} channels at the single-channel level with Na^+ as a charge carrier, increasing external pH increases the relative frequency of high conductance substates with a similar pK_a of ~8.5 (Chen et al., 1996). A possible target is the ring of glutamate residues within the channel, because mutation to glutamine made the channel behave as if it were protonated. Although glutamate has a pK_a of ~4.4, it was suggested for L-type Ca^{2+} channels that multiple hydrogen-bonded carboxylates may have a much higher pK_a than unpaired carboxylates (Chen et al. 1996). Assuming similar glutamate residues in the pore of CRAC channels, protonation of these amino acids could affect the currents through CRAC channels.

Possible Relation of CRAC Channels to TRP

Recently, homologues of the *Drosophila trp* gene have been identified in human (Wes et al., 1995; Birnbaumer et al., 1996; Zhu et al., 1996; Zitt et al., 1996). TRPC1A shares with CRAC channels the property of being activated by depletion of Ca^{2+} stores, but in contrast to CRAC channels, TRP channels are nonselective cation channels (Hardie and Minke 1992; Phillips et al., 1992; Hu et al., 1994; Vaca et al., 1994; Zitt et al., 1996). In the present study, we showed that CRAC channels are basically nonselective cation channels and obtain their Ca^{2+} selectivity by their affinity to Ca^{2+}. Therefore, CRAC channels may represent Ca^{2+}-selective variants of TRP channels. We anticipate that the biophysical characterization of permeation, rectifica-

tion, and block will be of value in identifying candidate genes encoding the CRAC channel.

Significance of I-V Shape and I-$[Ca^{2+}]_o$ for T-Cell Activation

The shape of the CRAC channel I-V relation is of considerable importance for $[Ca^{2+}]_i$ signaling, gene expression, and proliferation in T lymphocytes. In contrast to Ca^{2+} influx through voltage-gated Ca^{2+} channels, Ca^{2+} current through CRAC channels is reduced by membrane depolarization. Membrane depolarization resulting from elevated levels of external K^+ or by application of specific K^+ channel blockers inhibits T cell activation and Ca^{2+} signaling indirectly by reducing Ca^{2+} influx through CRAC channels (reviewed in Lewis and Cahalan, 1995). The inhibition is stronger than one might expect simply from the change in driving force $E_m - E_{Ca}$, because the I-V relation is not linear. To obtain an estimate of the Ca^{2+} influx at the resting potential compared with a fully depolarized cell, we analyzed relative inward current amplitudes at −60 and 0 mV, using cells with $NMDG^+$ inside to prevent contamination by outward currents. Ca^{2+} currents at −60 mV were 4.0 ± 0.7-fold larger than at 0 mV ($n = 5$). As a result of inward rectification mediated by Mg^{2+} block, depolarization near 0 mV would reduce Ca^{2+} influx through CRAC channels by 75%, to a level where existing Ca^{2+} pump mechanisms reduce the residual $[Ca^{2+}]_i$ to a level below that required for gene expression.

Since CRAC channels provide the trigger for activation of signaling pathways inside T cells leading to gene expression and activation or apoptosis, a low conductance channel may be beneficial to avoid inadvertent signaling. Because of its small volume and low resting $[Ca^{2+}]_i$ of 100 nM, a human T cell contains fewer than 10^4 free Ca^{2+} ions in cytoplasm. Even considering the ability of cytoplasm to buffer Ca^{2+}, a very small Ca^{2+} current (order of 1 pA) will result in a large change in $[Ca^{2+}]_i$. Thus, to control the rise in $[Ca^{2+}]_i$, it may be advantageous to limit Ca^{2+} influx through a CRAC channel to thousands rather than millions of ions per second. The low Ca^{2+} throughput may be seen in the very low single-channel conductance of a CRAC channel, as well as in the I-$[Ca^{2+}]_o$ relation.

The authors acknowledge the continued excellent assistance of Dr. Lu Forrest in cell culture.

This work was supported by National Institutes of Health grants NS-14609 and GM-41514.

Original version received 28 August 1997 and accepted version received 21 January 1998.

REFERENCES

Agus, Z.S., and M. Morad. 1991. Modulation of cardiac ion channels by magnesium. *Annu. Rev. Physiol.* 53:299–307.

Almers, W., and E.W. McCleskey. 1984. Non-selective conductance in calcium channels of frog muscle: calcium selectivity in single-file pore. *J. Physiol. (Camb.).* 353:585–608.

Almers, W., E.W. McCleskey, and P.T. Palade. 1984. A non-selective cation conductance in frog muscle membrane blocked by micromolar external calcium ions. *J. Physiol. (Camb.).* 353:565–583.

Armstrong, C.M., and J. Neyton. 1991. Ion permeation through calcium channels. A one-site model. *Ann. NY Acad. Sci.* 635:18–25.

Bara, M., A. Guiet-Bara, and J. Durlach. 1993. Regulation of sodium and potassium pathways by magnesium in cell membranes. *Magnes. Res.* 6:167–177.

Birnbaumer, L., X. Zhu, M. Jiang, G. Boulay, M. Peyton, B. Vannier, D. Brown, D. Platano, H. Sadeghi, E., Stefani, and M. Birnbaumer. 1996. On the molecular basis and regulation of cellular capacitative calcium entry: roles for Trp proteins. *Proc. Natl. Acad. Sci. USA.* 93:15195–15202.

Burnashev, N., A. Villarroel, and B. Sakmann. 1996. Dimensions and ion selectivity of recombinant AMPA and kainate receptor channels and their dependence on Q–R site residues. *J. Physiol. (Camb.).* 496:165–173.

Chen, X.H., I. Bezprozvanny, and R.W. Tsien. 1996 Molecular basis of proton block of L-type Ca^{2+} channels. *J. Gen. Physiol.* 108:363–374.

Clapham, D.E. 1996. TRP is cracked but is CRAC TRP? *Neuron.* 16: 1069–1072.

Crabtree, G.R., and N.A. Clipstone. 1994. Signal transmission between the plasma membrane and nucleus of T lymphocytes. *Annu. Rev. Biochem.* 63:1045–1083.

Dwyer, T.M., D.J. Adams, and B. Hille. 1980. The permeability of the endplate channel to organic cations in frog muscle. *J. Gen. Physiol.* 75:469–492.

Ellinor, P.T., J. Yang, W.A. Sather, J.F. Zhang, and R.W. Tsien. 1995. Ca^{2+} channel selectivity at a single locus for high-affinity Ca^{2+} interaction. *Neuron.* 15:1121–1132.

Fanger, C.M., M. Hoth, G.R. Crabtree, and R.S. Lewis. 1995. Characterization of T cell mutants with defects in capacitative calcium entry: genetic evidence for the physiological roles of CRAC channels. *J. Cell Biol.* 131:655–667.

Hamill, O.P., A. Marty, E. Neher, B. Sakman, and F.J. Sigworth. 1981. Improved patch-clamp techniques for high-resolution current recording form cells and cell-free membrane patches. *Pflügers Arch.* 391:85–100.

Hardie, R.C., and B. Minke. 1992. The trp gene is essential for a light-activated Ca^{2+} channel in *Drosophila* photoreceptors. *Neuron.* 8:643–651.

Hess, P., J.B. Lansman, and R.W. Tsien. 1986. Calcium channel selectivity for divalent and monovalent cations. *J. Gen. Physiol.* 88: 293–319.

Hess, P., and R.W. Tsien. 1984. Mechanism of ion permeation through calcium channels. *Nature.* 309:453–456.

Hoth, M. 1995. Calcium and barium permeation through calcium release-activated calcium (CRAC) channels. *Pflügers Arch.* 430: 315–322.

Hoth, M., and R. Penner. 1992. Depletion of intracellular calcium

stores activates a calcium current in mast cells. *Nature.* 355:353–356.

Hoth, M., and R. Penner. 1993. Calcium release-activated calcium current in rat mast cells. *J. Physiol. (Camb.).* 465:359–386.

Hu, Y., L. Rajan, and W.P. Schilling. 1994. Ca^{2+} signaling in Sf9 insect cells and the functional expression of a rat brain M5 muscarinic receptor. *Am. J. Physiol.* 266:C1736–C1743.

Kaibara, M., and M. Kameyama. 1988. Inhibition of the calcium channel by intracellular protons in single ventricular myocytes of the guinea-pig. *J. Physiol. (Camb.).* 403:621–640.

Klöckner, U., and G. Isenberg. 1994. Intracellular pH modulates the availability of vascular L-type Ca^{2+} channels. *J. Physiol. (Camb.).* 103:647–663.

Kostyuk, P.G., and O.A. Krishtal. 1977. Effects of calcium and calcium-chelating agents on the inward and outward current in the membrane of mollusc neurons. *J. Physiol. (Camb.).* 270:569–580.

Kostyuk, P.G., S.L. Mironov, and Y.M. Shuba. 1983. Two ion-selecting filters in the calcium channel of the somatic membrane of mollusc neurons. *J. Membr. Biol.* 76:83–93.

Kuo, C., and P. Hess. 1993. Block of the L-type Ca^{2+} channel pore by external and internal Mg^{2+} in rat phaechromocytoma cells. *J. Physiol. (Camb.).* 466:683–706.

Lansman, J.B., P. Hess, and R.W. Tsien. 1986. Blockade of current through single calcium channels by Cd^{2+}, Mg^{2+}, and Ca^{2+}. Voltage and concentration dependence of calcium entry into the pore. *J. Gen. Physiol.* 88:321–347.

Lepple-Wienhues, A., and M.D. Cahalan. 1996. Conductance and permeation of monovalent cations through depletion-activated Ca^{2+} channels (I_{CRAC}) in Jurkat T cells. *Biophys. J.* 71:787–794.

Lewis, R.S., and M.D. Cahalan. 1989. Mitogen-induced oscillations of cytosolic Ca^{2+} and transmembrane Ca^{2+} current in human leukemic T cells. *Cell Regul.* 1:99–112.

Lewis, R.S., and M.D. Cahalan. 1995. Potassium and calcium channels in lymphocytes. *Annu. Rev. Immunol.* 13:623–653.

Lewis, R.S., R.E. Dolmetsch, and A. Zweifach. 1996. Positive and negative regulation of depletion-activated calcium channels by calcium. *Soc. Gen. Physiol. Ser.* 51:241–254.

Lewis, R.S., P. Ross, and M.D. Cahalan. 1993. Chloride channels activated by osmotic stress in T lymphocytes. *J. Gen. Physiol.* 101: 801–826.

Malayev, A., and D.J. Nelson 1995. Extracellular pH modulates the Ca^{2+} current activated by depletion of intracellular Ca^{2+} stores in human macrophages. *J. Membr. Biol.* 146:101–111.

McCleskey, E.W., and W. Almers. 1985. The Ca channel in skeletal muscle is a large pore. *Proc. Natl. Acad. Sci. USA.* 82:7149–7153.

Negulescu, P.A.N., N. Shastri, and M.D. Cahalan. 1994. Intracellular calcium dependence of gene expression in single T lymphocytes. *Proc. Natl. Acad. Sci. USA.* 91:2873–2877.

Neher, E. 1988. The influence of intracellular Ca^{2+} concentration on degranulation of dialyzed mast cells from rat peritoneum. *J. Physiol. (Camb.).* 395:193–214.

Nichols, C.G., and A.N. Lopatin. 1997 Inward rectifier potassium channels. *Annu. Rev. Physiol.* 59:171–191.

Nowak, L., P. Bregestovski, P. Ascher, A. Herbet, and A. Prochiantz. 1984. Magnesium gates glutamate-activated channels in mouse central neurones. *Nature (Camb.).* 307:462–465.

Parekh, A.B., and R. Penner. 1996. Regulation of store-operated calcium currents in mast cells. *Soc. Gen. Physiol. Ser.* 51:231–239.

Phillips, A.M., A. Bull, and L.E. Kelly. 1992. Identification of a *Drosophila* gene encoding a calmodulin-binding protein with homology to the trp phototransduction gene. *Neuron.* 8:631–642.

Premack, B.A., T.V. McDonald, and P. Gardner. 1994. Activation of Ca^{2+} current in Jurkat T cells following the depletion of Ca^{2+} stores by microsomal Ca^{2+}-ATPase inhibitors. *J. Immunol.* 152: 5226–5240.

Pusch, M. 1990. Open-channel block of Na^{+} channels by intracellular Mg^{2+}. *Eur. Biophys. J.* 18:317–326.

Vaca, L., W.G. Sinkins, Y. Hu, D.L. Kunze, and W.P. Schilling. 1994. Activation of recombinant trp by thapsigargin in Sf9 insect cells. *Am. J. Physiol.* 267:C1501–C1505.

Vandenberg, C.A. 1987. Inward rectification of a potassium channel in cardiac ventricular cells depends on internal magnesium ions. *Proc. Natl. Acad. Sci. USA.* 84:2560–2564.

Wes, P.D., J. Chevesich, A. Jeromin, C. Rosenberg, G. Stetten, and C. Montell. 1995. TRPC1, a human homolog of a *Drosophila* store-operated channel. *Proc. Natl. Acad. Sci. USA.* 92:9652–9656.

Woodhull, A.M. 1973. Ionic blockage of sodium channels in nerve. *J. Gen. Physiol.* 61:687–708.

Zhang, L., and M.A. McCloskey. 1995. Immunoglobulin E receptor-activated calcium conductance in rat mast cells. *J. Physiol. (Camb.).* 483:59–66.

Zhu, X., M. Jiang, M. Peyton, G. Boulay, R. Hurst, E. Stefani, and L. Birnbaumer. 1996. trp, a novel mammalian gene family essential for agonist-activated capacitative Ca^{2+} entry. *Cell.* 85:661–671.

Zitt, C., A. Zobel, A.G. Obukhov, C. Harteneck, F. Kalkbrenner, A. Lückhoff, and G. Schultz. 1996. Cloning and functional expression of a human Ca^{2+}-permeable cation channel activated by calcium store depletion. *Neuron.* 16:1189–1196.

Zweifach, A., and R.S. Lewis. 1993. Mitogen-regulated Ca^{2+} current of T lymphocytes is activated by depletion of intracellular Ca^{2+} stores. *Proc. Natl. Acad. Sci. USA.* 90:6295–6299.

Zweifach, A., and R.S. Lewis. 1996. Calcium-dependent potentiation of store-operated calcium channels in T lymphocytes. *J. Gen. Physiol.* 107:597–610.